

## PARAMETER SENSITIVITY OF UNDERGROUND DC MEASUREMENTS

Ákos GYULAI\*

Parameter sensitivities are useful for comparing underground dc techniques and for planning surveys. After defining the thickness (depth) sensitivity and the resistivity sensitivity, the parameter sensitivity functions for different deposit models (coal, bauxite) are presented then, based on these, some characteristic features of underground measurements.

**Keywords:** electric methods, resistivity, in-mine geophysics, direct current methods, parameter sensitivity

### 1. Introduction

Various in-mine geophysical, among them dc, methods have been developed to determine the rock and deposit parameters and the disturbances of deposits. Usually, reliable geological interpretation required by the mining industry can be achieved by the combined application of several methods. The efficient use of these methods is possible if the resolution of the individual methods is known and utilized. Selection of the methods making up the optimum measurement set is harder and more complex than in surface geophysical surveys, because underground measurements are carried out in a whole space; in other words, the investigation can be directed downwards, upwards or laterally. A further drawback is that up till now we have far less empirical experience.

### 2. Determination of the layer parameters

Underground geoelectric measurements have several new possibilities. If one gets closer to the object to be investigated not only can geological deviations undetectable by the known surface methods be revealed but there are also novel possibilities for field generation and measurement. Using these possibilities the sensitivity of geoelectric surveys, thus their efficiency, can be increased by several orders of magnitude.

Underground measurements also offer the special possibility of measuring with vertical dipoles in drifts and boreholes. Soundings can be carried out at

\* Technical University for Heavy Industry, Department of Geophysics, Miskolc–Egyetemváros, H-3515, Hungary

Manuscript received (revised version): 21 July, 1989

several levels below ground. A further underground method is the transillumination of the space between drifts, between a drift and a drillhole, and between drillholes.

One type of survey task is represented by investigating the seam itself by determining the seam thickness, seam disturbances and seam quality. Geoelectric seam-sounding and seam-transillumination methods can solve these tasks [CSÓKÁS 1974, CSÓKÁS et al. 1986, DOBRÓKA et al. 1987b, KIRÁLY-SZIGETI 1985].

Investigation of the layers over- and underlying the seam represents an other group of tasks. The geoelectrical methods used for these purposes can be summarized under drift-sounding and -profiling [GYULAI 1979, GYULAI 1985, SZABÓ-GÉRESI 1983].

To determine the layer parameters of a coal-bearing complex the above methods are combined [BREITZKE et al. 1987]. Several possibilities offer themselves for comparing different methods. One of the procedures is to compare the penetration depths [EGERSZEGI 1980]. Another way of comparison is to examine the sounding curves of various models. Let us choose this method first to compare seam-sounding, roof-sounding and floor-sounding. *Figure 1* shows sounding curves calculated for a five-layer model with different seam resistivities. (It is assumed that the thickness of the first layer,  $M_1$ , can be considered infinite). It can be seen that for a vertical dipole (Fig. 1/c) the apparent resistivity values ( $\varrho_a$ ) increase when the resistivity of the seam ( $\varrho_2$ ) increases, and this effect is even more pronounced at larger separations. In roof- (Fig. 1/a) and floor-soundings (Fig. 1/b) a considerably smaller increase is experienced than in the previous case.

Changes caused by an increase in the seam resistivity can be better observed in *Fig. 2*, which shows the deviations from the quasi-four-layer model. Differences between the different electrode arrays can be seen as well. Seam-sounding (Fig. 2/c) is very sensitive to changes in seam resistivity. In the case of drift-soundings, that one is more sensitive to the changes in seam resistivity which is measured on the side of the host rock that has higher resistivity.

### 3. The parameter sensitivities

Different electrode arrays can most simply be compared if the measure of variations in apparent resistivity curves caused by the changes in layer parameters is examined. That array is considered to be the most favourable which exhibits the highest sensitivity.

The relation between apparent resistivity ( $\varrho_a$ ) and parameter ( $M_i$ ,  $\varrho_i$ ) changes can be defined by the equations

$$\psi_i = \frac{\partial \varrho_a}{\partial M_i} \frac{M_i}{\varrho_a} = \frac{\partial(\ln \varrho_a)}{\partial(\ln M_i)} \quad (1)$$

and

$$\varphi_i = \frac{\partial \varrho_a}{\partial \varrho_i} \frac{\varrho_i}{\varrho_a} = \frac{\partial(\ln \varrho_a)}{\partial(\ln M_i)} \quad (2)$$

$\psi_i$  and  $\varphi_i$  are the so-called thickness and resistivity sensitivities [DOBROKA et al. 1987a]. The sensitivities can be described by the following formulae as well:

$$\psi^* = \frac{\partial \varrho_a}{\partial M_i} \frac{1}{\varrho_a} = \frac{\partial(\ln \varrho_a)}{\partial M_i} \quad (3)$$

and

$$\varphi^* = \frac{\partial \varrho_a}{\partial \varrho_i} \frac{1}{\varrho_a} = \frac{\partial(\ln \varrho_a)}{\partial \varrho_i} \quad (4)$$

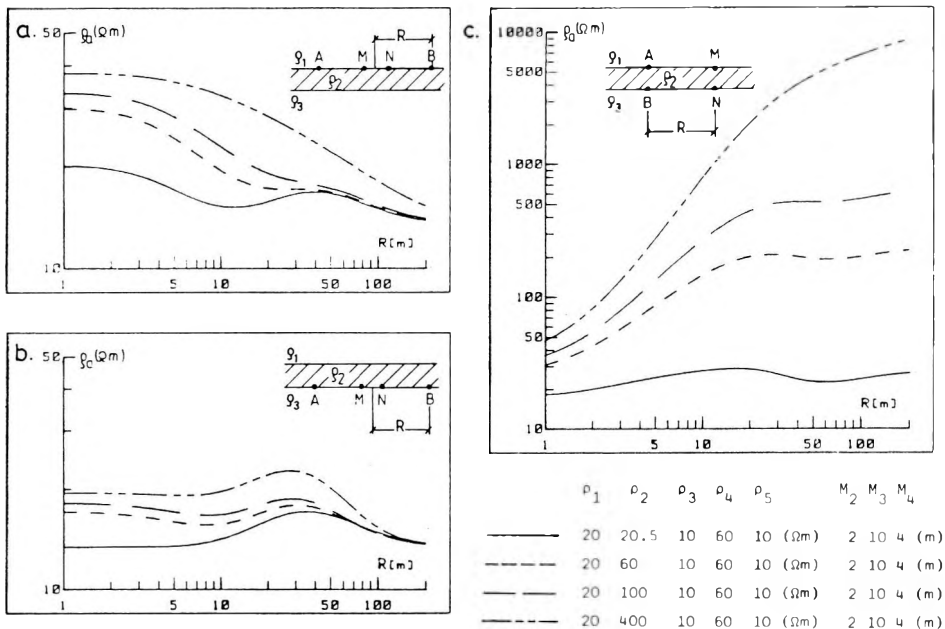


Fig. 1. Apparent resistivity ( $\varrho_a$ ) curves for five-layer models. Basis for comparison: A quasi-four-layer ( $\varrho_1 \sim \varrho_2$ ) model. Model parameters can be seen in the lower right corner, the electrode arrays are shown near the respective curve  
 a) Roof-sounding; b) Floor-sounding; c) Seam-sounding

1. ábra. Látszólagos fajlagos ellenállás ( $\varrho_a$ ) görbék ötréteges modellekre. Összehasonlítási alap: a négyrétegesnek tekinthető ( $\varrho_1 \sim \varrho_2$ ) modell. A modell paraméterek a jobb alsó sarokban, az elektróda elrendezések a megfelelő szondázási görbék mellett láthatók  
 a) Fedőszondázás; b) Feküszondázás; c) Teleszondázás

Рис. 1. Кривые кажущихся удельных сопротивлений ( $\varrho_a$ ) для пятислойных моделей. Основа для сопоставлений: модель ( $\varrho_1 \sim \varrho_2$ ), которая может рассматриваться в качестве четырехслойной. Параметры модели – в правом нижнем углу, при кривых зондирования, соответствующих установке.

a) Зондирование кровли; b) Зондирование почвы; c) Зондирование пласта

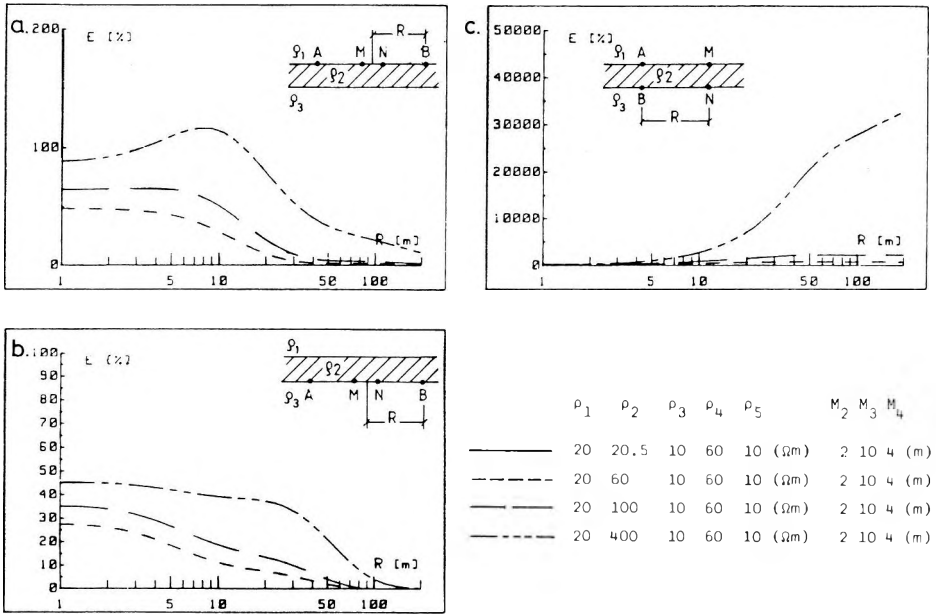


Fig. 2. Deviation ( $E$ ) of the sounding curves shown in Fig. 1 from the quasi-four-layer curve which contains no coal seam

a) Roof-sounding; b) Floor-sounding; c) Seam-sounding

2. ábra. Az 1. ábrán látható szondázási görbék eltérése ( $E$ ) a szénréteget nem tartalmazó, négyrétegesnek tekinthető görbétől

a) Fedőszondázás; b) Fekűszondázás; c) Telepszondázás

Рис. 2. Отклонение ( $E$ ) кривой зондирования на рис. 1 от кривой разреза без угольного пласта, которая может рассматриваться в качестве четырехслойной.

a) Зондирование кровли; б) Зондирование почвы; в) Зондирование пласта

or by the quantities

$$m = \frac{\partial \lg Q_a}{\partial M_i} \tag{5}$$

$$n = \frac{\partial \lg Q_a}{\partial \rho_i} \tag{6}$$

Figure 3 shows such curves. When sounding curves are interpreted they are compared in a  $\lg Q_a - \lg AB/2$  system thus it is expedient to use the quantities defined by Eqs. (1)–(4) which contain logarithmic gradient. The use of formulae (1) and (2) is the most advantageous because these characterize the relation between the apparent resistivity function and the parameter changes in a dimensionless form. It should be noted that in inversion methods either relations (1) and (2) or (3) and (4) are used [KOEFOED 1979]. The information matrix which

is used to characterize the reliability of statistical interpretation [GOLC'MAN 1976, SALÁT et al. 1982] is derived from derivatives (1) and (2).

It can be seen in Fig. 3 that functions  $m$ ,  $\psi^*$  and  $\psi$  change sign at small thickness. This is of interest to us for two reasons: on the one hand, there exists a critical thickness at every separation in the vicinity of which change in thickness does not manifest itself in apparent resistivities, on the other hand, at thicknesses smaller or larger than this a change in thickness may cause a change of opposite direction in apparent resistivity.

In addition it can be seen in the figure too that although the depth sensitivity changes, there exists a depth interval in which it can be considered constant. For example, for function  $\psi$ ,  $\bar{\psi}$  equals  $-0.46$  between 12 and 33 m, where  $\bar{\psi}$  and similarly  $\bar{\psi}^*$  and  $\bar{m}$ , is the mean value of  $\psi$  in the given interval. It means that in this thickness (depth) interval a 0.46% decrease in apparent resistivity suggests a 1% increase in thickness.

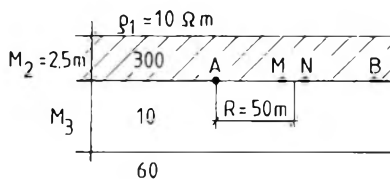
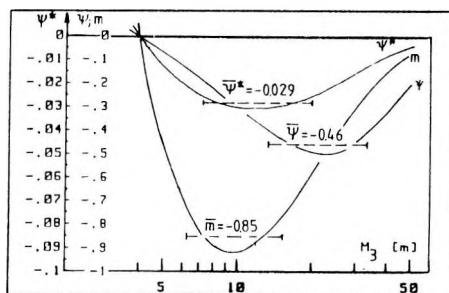
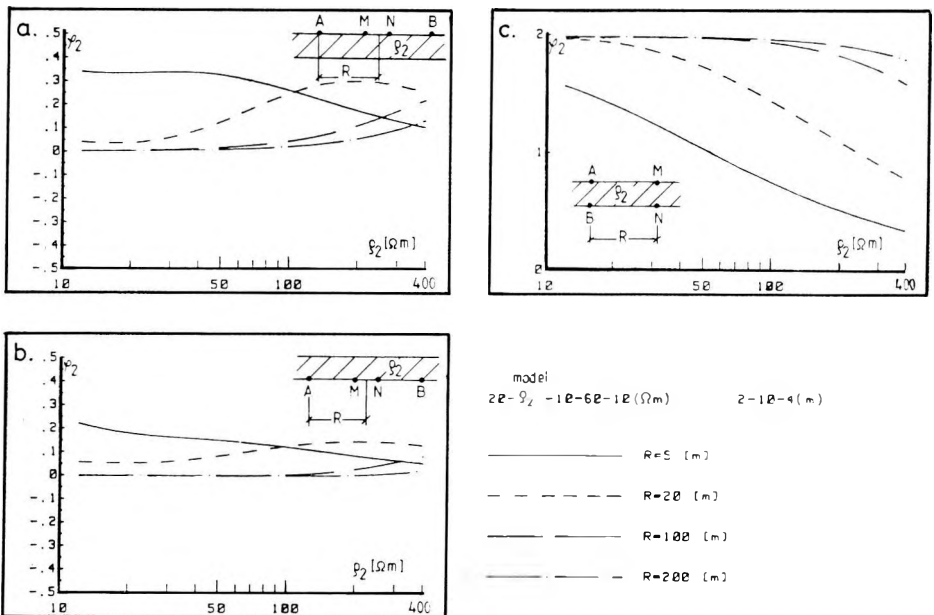


Fig. 3. Thickness sensitivity ( $\psi$ ,  $\psi^*$ ,  $m$ ) curves of the model and electrode array shown in the figure as a function of the thickness of the layer underlying the coal seam ( $M_3$ )

3. ábra. Vastagság érzékenység ( $\psi$ ,  $\psi^*$ ,  $m$ ) görbék az ábrán látható modellre és elektróda elrendezésre, a széntelep alatti fekvőréteg vastagságának ( $M_3$ ) függvényében.

Рис. 3. Кривые чувствительности к мощности ( $\psi$ ,  $\psi^*$ ,  $m$ ) для модели и установки, изображенных на рисунке, как функция мощности слоя ( $M_3$ ), подстилающего угольный пласт.

Let us see, based on the sensitivities defined by (1) and (2), what kind of further statements can be made concerning the already mentioned model and soundings. In *Fig. 4* the sensitivity to the seam resistivity can be seen as a function of the seam resistivity ( $\rho_2$ ) for different arrays. The low sensitivity of the floor-sounding can be observed: at a separation of 100 m and ( $\rho_2$ ) = 300  $\Omega\text{m}$   $\phi_2$  is less than 0.05. It means that a 10% increase in the seam resistivity causes a 0.5% increase in the apparent resistivity. The sensitivity of the roof-sounding is twice as high as the previous one. The  $\phi_2$  sensitivity of the seam-sounding is outstandingly high; in an optimum case  $\phi_2$  is 2. This feature of the measurement with vertical dipoles becomes apparent at large separations, but the sensitivity already reaches the favourable value of 1 at about  $R=5$  m. It is important to note that the high resistivity sensitivity related to the layer situated between the vertical dipoles can be observed at low resistivity contrasts, too.



*Fig. 4.* Resistivity sensitivity ( $\phi$ ) curves at four separations as a function of coal seam resistivity ( $\rho_2$ )

a) Roof-sounding; b) Floor-sounding; c) Seam-sounding

4. ábra. Fajlagosellenállás érzékenység ( $\phi$ ) görbék négy különböző terítési távolságra, a széntelep ellenállásának ( $\rho_2$ ) függvényében

a) Fedőszondázás; b) Feküszondázás; c) Telepszondázás

*Рис. 4.* Кривые чувствительности к сопротивлению ( $\phi$ ) для четырех различных разнесов, как функция мощности ( $M_2$ ) угольного пласта.

a) Зондирование кровли; б) Зондирование почвы; в) Зондирование пласта

Figure 5 shows the seam thickness sensitivity ( $\psi_2$ ). It is valid of the thickness sensitivity, too, that the sensitivity of the roof-sounding is twice as high as that of the floor-sounding. Thickness sensitivity can be calculated from the apparent resistivities of the vertical dipole measurement, too, but completely different results will be obtained. This kind of sensitivity is approximately the same as the resistivity. If the resistivity of the seam is high ( $\rho_2 = 400 \Omega\text{m}$ ) the sensitivity approximates the value of 2 in thin seams and only at large separations. High thickness sensitivity means that the vertical dipole array can advantageously be applied to investigate the thickness variations of the seam between the electrodes.

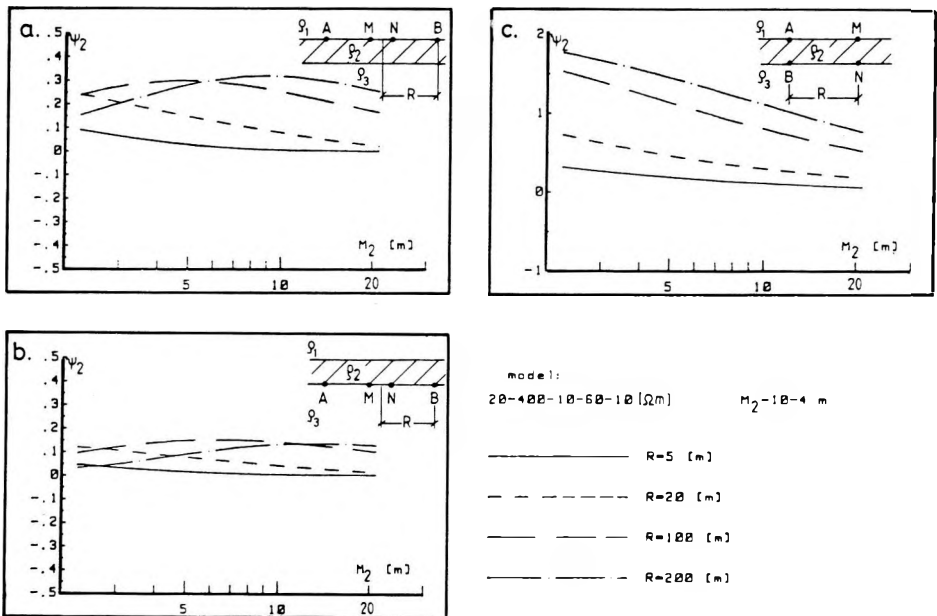


Fig. 5. Thickness sensitivity ( $\psi$ ) curves at four separations as a function of coal seam thickness ( $M_2$ )

a) Roof-sounding; b) Floor-sounding; c) Seam-sounding

5. ábra. Vastagság érzékenység ( $\psi$ ) görbék négy különböző terítési távolságra, a széntelep vastagságának ( $M_2$ ) függvényében

a) Fedőszondázás; b) Fekűszondázás; c) Telepszondázás

Рис. 5. Кривые чувствительности к мощности ( $\psi$ ) для четырех различных разносов, как функция мощности ( $M_2$ ) угольного пласта.

a) Зондирование кровли; б) Зондирование почвы; в) Зондирование пласта

In Figs. 6. and 7. the resistivity sensitivities of the measurements performed in a bauxite deposit can be seen. The measurements are carried out somewhere within the deposit and the effect of the lower (floor side) and the upper part (roof side) of the deposit is examined. Fig. 6 shows the sensitivity to the floor side of the deposit, Fig. 7 that to the roof side. The sensitivity of the Schlumberger array at larger separations ( $R = 50, 100$  m) hardly differs from zero in Fig. 6; this kind of measurement is insensitive to changes in the high resistivity floor side. In the case of deposit changes in the roof side  $\varphi_2$  is greater than 0.5 at the same separations and it increases with the resistivity of this deposit part (contrary to the previous case). At shorter separations ( $R = 10, 20$  m) the sensitivities are the same in both directions. It is noted that at larger separations the sensitivity of the vertical dipole array is  $\sim 1.5$ , in addition,  $\varphi_3$  is positive in the  $R = 10 - 100$  m interval. Sensitivities related to the deposit part outside the vertical dipoles hardly differ from zero at shorter separations (10, 20 m) in Fig. 7; at larger separations (50, 100 m) the sensitivity increases though it is opposite in sign compared to the sensitivity related to the deposit part between the vertical dipoles.

It can be seen that the investigation can be directed downwards or upwards even if the complex is not cut in two parts by a high resistivity layer (e.g. coal seam). Further it can be stated, too, that the sensitivity related to the layer between the vertical dipoles is high in every case thus this array can favourably be applied not only to coal seam models (seam-sounding).

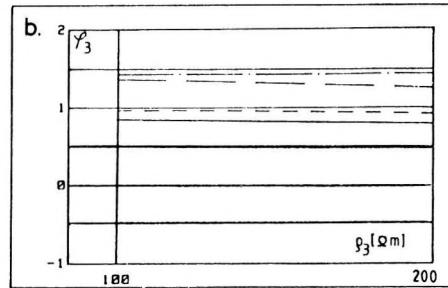
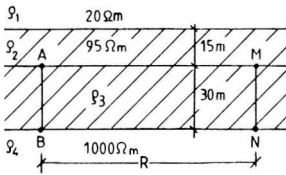
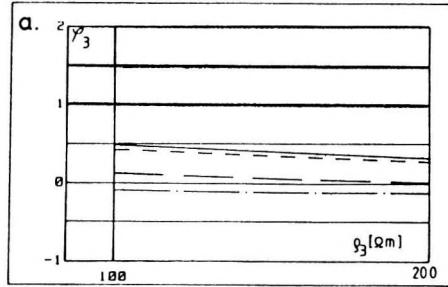
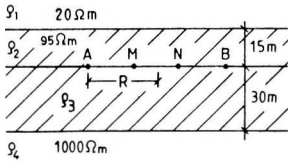
Figure 8. shows underlying layer thickness sensitivity functions for a coal seam model. This model corresponds to a case in which a water saturated sand layer ( $\rho_4 = 60 \Omega\text{m}$ ) can be found in the underlying sequence and this is separated from the coal seam ( $\rho_2$ ) by a low resistivity clay layer, the so-called protective layer.

Let us take a closer look at the behaviour of the sensitivity functions:

- for roof-sounding  $\psi_3 \sim 0$ , therefore this is unsuitable for investigating the protective layer,
- for floor-sounding at  $R = 5$  m and  $M_3 \sim 3$  m the sensitivity is favourable:  $\psi_3 = -0.5$  but it rapidly decreases with increasing thickness of the protective layer; the optimum of the sensitivity function is at  $M_3 = 8 - 10$  m for  $R = 20$  m:  $\psi_3 \sim 0.4$ ; the sensitivity has a critical point at  $R = 50$  m,  $M_3 = 10$  m ( $\psi_3 \sim 0$ ) and the sensitivity changes sign; at  $R = 100$  m,  $\psi_3$  is positive for  $M_3 = 2 - 20$  m, i.e. when the thickness of the low resistivity layer increases the apparent resistivity increases, too (contrary to our expectation),
- sensitivities of the seam-sounding fall between  $-0.2$  and  $0.2$ , they are positive at  $R = 50, 100$  m in the thickness interval under consideration.

The effect of variation in the deposit thickness for a bauxite model is shown in Figs. 9, 10 and 11. for different drift-sounding arrays. These curves were calculated for a dolomite basement having a resistivity of  $2500 \Omega\text{m}$ . It can already be seen in Fig. 9 that from the resistivity sounding curves of the model containing a 20 m or 30 m thick bauxite layer the largest deviation appears in the curves of the dipole-dipole array. The highest value of the deviation is 10%



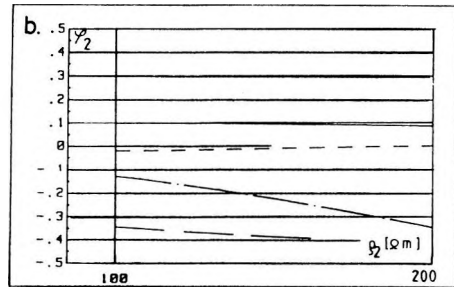
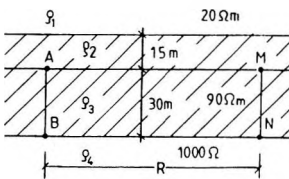
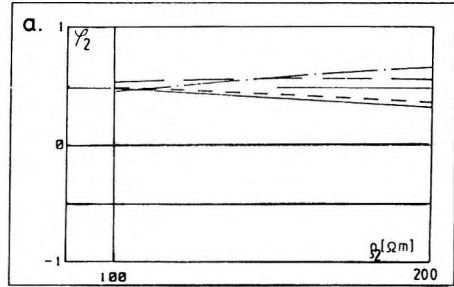
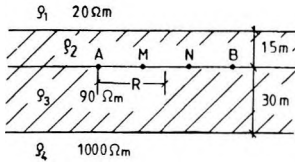


- R=100 [m]
- - - - - R=200 [m]
- · - · - R=500 [m]
- - - - - R=1000 [m]

Fig. 6. Resistivity sensitivity ( $\phi$ ) curves of a bauxite deposit model, at four separations, as a function of the resistivity of the lower, floor-side 30 m thick part of the deposit  
 a) Schlumberger sounding carried out in the roof-side part of the deposit, at the boundary between the constant and variable resistivity parts  
 b) Sounding carried out with vertical dipoles spanning the 30 m thick, floor-side, variable resistivity part of the deposit

6. ábra. Fajlagosellenállás érzékenység ( $\phi$ ) görbék egy bauxittelep modellre, négy terítési távolságra, a telep alsó, fekü felőli, 30 m vastag része ellenállásának függvényében  
 a) A telep fedő oldali részében, az állandó és változó ellenállású részt elválasztó felületen végzett Schlumberger-szondázás  
 b) A telep fekü oldali, változó ellenállásúnak tekintett, 30 m vastag részét átfogó függőleges dipólokkal végzett szondázás

Рис. 6. Кривые чувствительности к сопротивлению ( $\phi$ ) для модели бокситовой залежи при четырех различных разносах, как функция сопротивления нижней, припочвенной части залежи мощностью 30 м.  
 а) Зондирование установкой Шлюмберже, выполненное в прикровельной части залежи, на поверхности, разделяющей области постоянных и переменных сопротивлений.  
 б) Зондирование вертикальными диполями, охватывающими припочвенную часть залежи мощностью 30 м, рассматриваемую как область переменных сопротивлений.



- R=10 (m)
- R=20 (m)
- · - · - R=50 (m)
- R=100 (m)

Fig. 7. Resistivity sensitivity ( $\varphi$ ) curves of a bauxite deposit model, at four separations, as a function of the resistivity of the upper, roof-side, 15 m thick part of the deposit  
 a) Schlumberger sounding carried out in the roof-side part of the deposit, at the boundary between the constant and variable resistivity parts  
 b) Sounding carried out with vertical dipoles spanning the 30 m thick floor-side, 90 Ωm resistivity part of the deposit

7. ábra. Fajlagosellenállás érzékenység ( $\varphi$ ) görbék egy bauxittelép modellre, négy terítési távolságra, a telep felső, fedő felőli, 15 m vastag része ellenállásának függvényében  
 a) A telep fedő oldali részében, a változó és állandó ellenállású részt elválasztó felületen végzett Schlumberger-szondázás  
 b) A telep fekü oldali, 90 Ωm fajlagosellenállásúnak tekintett, 30 m vastag részét átfogó függőleges dipólokkal végzett szondázás

Рис. 7. Кривые чувствительности к сопротивлению ( $\varphi$ ) для модели бокситовой залежи при четырех различных разносах, как функция сопротивления верхней, прикровельной части залежи мощностью 15 м.  
 а) Зондирование установкой Шлюмберже, выполненное в прикровельной части залежи, на поверхности, разделяющей области постоянных и переменных сопротивлений.  
 б) Зондирование вертикальными диполями, охватывающими припочвенную часть залежи мощностью 30 м, рассматриваемую как область с сопротивлением в 90 ом-м.

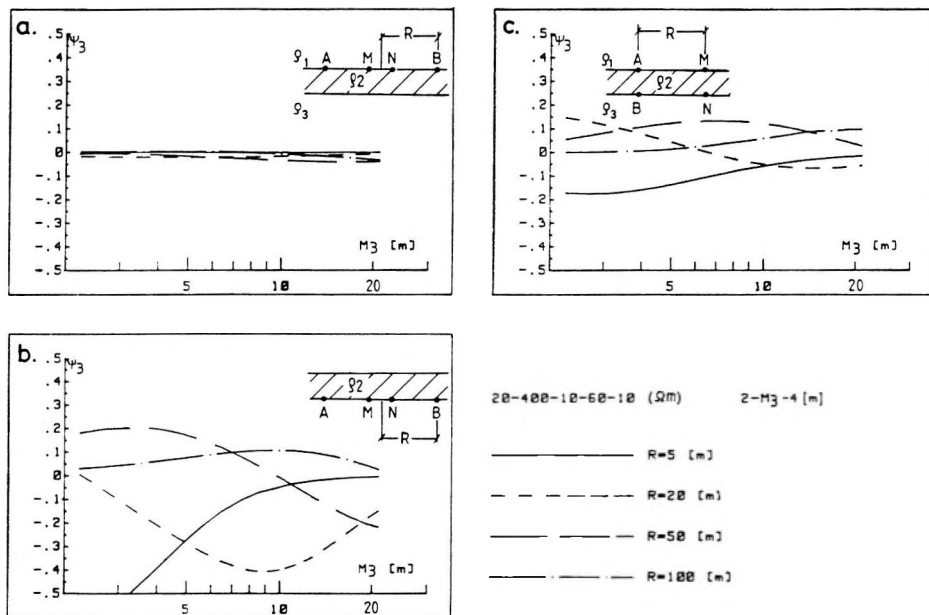


Fig. 8. Thickness sensitivity ( $\psi$ ) curves of a model with a coal seam, at four separations, as a function of the thickness of the layer underlying the coal seam ( $M_3$ )  
 a) Roof-sounding; b) Floor-sounding; c) Seam-sounding

8. ábra. Vastagság érzékenység ( $\psi$ ) görbék egy széntelepessel, négy terítési távolságra, a széntelep alatti feküreg vastagságának ( $M_3$ ) függvényében  
 a) Fedőszondázás; b) Feküszondázás; c) Teleszondázás

Рис. 8. Кривые чувствительности к мощности ( $\psi$ ) для модели угольного пласта при четырех различных разносах, как функция мощности ( $M_3$ ) слоя, подстилающего угольный пласт.

a) Зондирование кровли; б) Зондирование почвы; в) Зондирование пласта

for the two-electrode array (AM), 15% for the Schlumberger array (AMNB) and 20% for the dipole-dipole array (ABNM) (Fig. 10). The various thickness sensitivities are shown in Fig. 11. The sensitivity is unfavourable for the Schlumberger array, at  $R=100$  m in the depth interval of 15–25 m,  $|\psi| \leq 0.05$  (Fig. 11/b). Such little values of sensitivity occur for other arrays as well (Figs. 11/a, 11/c).

Figure 12. shows sounding and sensitivity curves for different levels of measurement. Based on the apparent resistivity curves we would expect that the sensitivity conditions for detecting a high resistivity layer (basement) are most favourable if the level of measurement is as close to it as possible. (The effect of the high resistivity layer can unambiguously be seen in curve 4 only.) The sensitivity curves demonstrate that the sensitivity does not change observably by changing the level of measurement at  $AB/2 = 5$  and 10 m. At  $AB/2 = 20$  and 50 m, however, the sensitivities are different for each level.

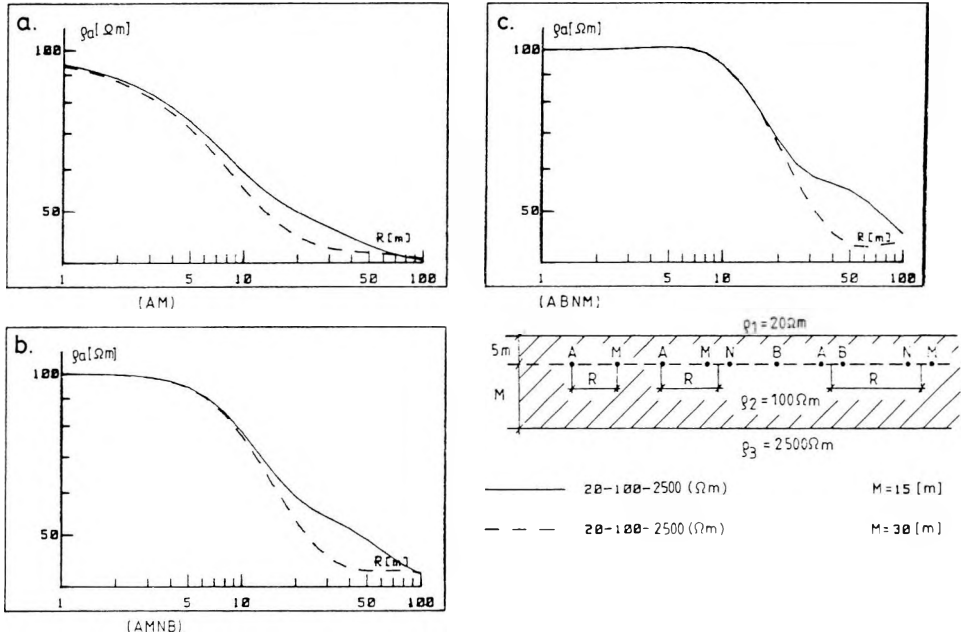


Fig. 9. Sounding curves for measurements carried out within a bauxite deposit, 5 m below the overlying layer. The high resistivity basement is 15 and 30 m below the level of measurements  
 a) Roof-sounding; b) Floor-sounding; c) Seam-sounding

9. ábra. Szondázási görbék a bauxitlepen belül, a fedőtől 5 m-re végzett mérésekre.

A nagyellenállású fekvő a mérés szintje alatt ( $M$ ) 15, illetve 30 m-re van  
 a) Kételektrodás; b) Schlumberger; c) Dipól-dipól elrendezés

Рис. 9. Кривые зондирования для измерений, выполненных в пределах бокситовой залежи, на расстоянии 5 м от кровли. Высокоомная почва находится ниже уровня измерений ( $M$ ) на 15 и 30 м.

a) Двухэлектродная установка; б) Установка Шлюмберже; в) Установка диполь-диполь

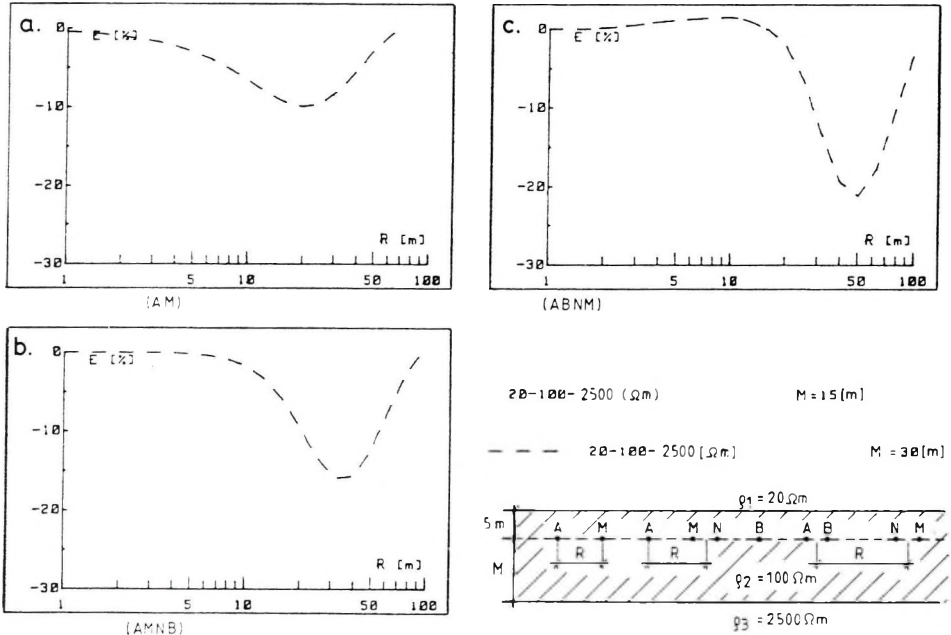


Fig. 10. Deviation ( $E$ ) curves of the sounding curves shown in Fig. 9

a) Two-electrode; b) Schlumberger; c) Dipole-dipole array

10. ábra. A 9. ábrán látható szondázási görbék eltérés ( $E$ ) görbéi

a) Kételektrodás-; b) Schlumberger-; c) Dipól-dipól elrendezés

Рис. 10. Кривые отклонений ( $E$ ) кривых зондирования на рис. 9.

a) Двухэлектродная установка; б) Установка Шлюмберже; в) Установка диполь-диполь

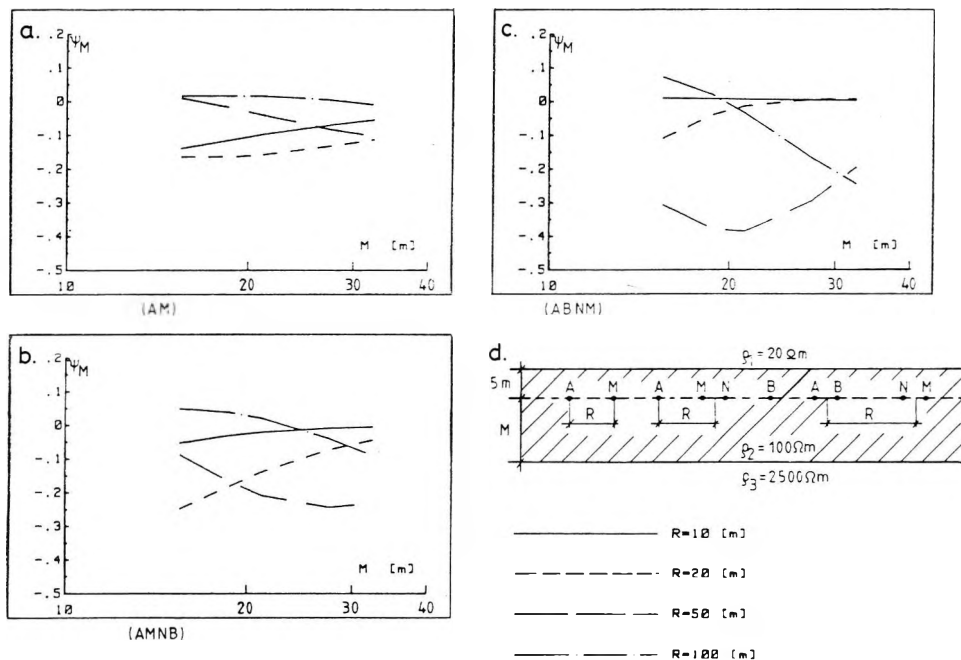


Fig. 11. Thickness sensitivity ( $\psi$ ) curves obtained for the model shown in Fig. 9 as a function of separation between the measurement level and basement ( $M$ ), for four electrode separations  
 a) Two-electrode; b) Schlumberger; c) Dipole-dipole array

11. ábra. A 9. ábrán látható modell esetén kapott vastagság érzékenység ( $\psi$ ) görbék a fektávolság ( $M$ ) függvényében, négy terítési távolságra  
 a) Kételektrodás; b) Schlumberger-; c) Dipól-dipól elrendezés

Рис. 11. Кривые чувствительности к мощности ( $\psi$ ) для модели рис. 9 как функция расстояния до почвы ( $M$ ) при четырех различных разносах.  
 а) Двухэлектродная установка; б) Установка Шлюмберже; в) Установка диполь-диполь

In the sensitivity curves for  $R=20$  m and 50 m we have marked those points which represent the thicknesses belonging to the respective levels. By connecting these points (dotted line) the curve showing the variation of sensitivities for different levels of measurement is obtained. It is mentioned that at  $R=20$  m (and for a bauxite thickness of 15 m) the sensitivity is highest at the 2nd level and lowest at the 4th level.

#### 4. Summary

In the planning of underground measurements the sensitivities are essential parameters. The basic concept of planning is that a measuring technique and separation should be utilized whose sensitivity is high in relation to the layer parameter to be studied and low in relation to the others. Based on the ex-

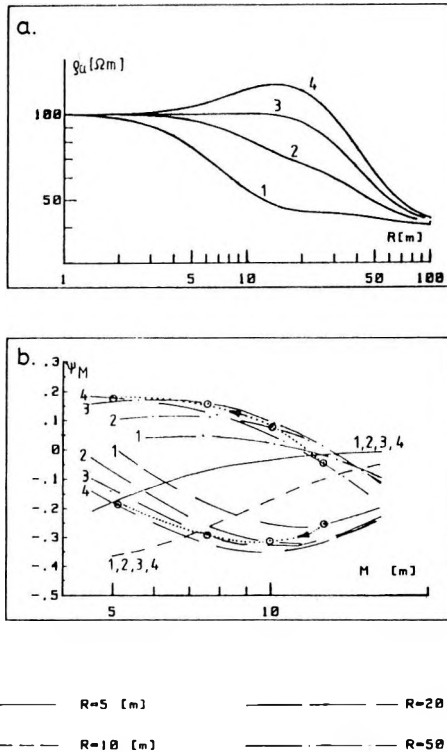


Fig. 12. Schlumberger soundings carried out at different levels above the high resistivity basement within a 15 m thick bauxite layer

a) Apparent resistivity ( $\rho_a$ ) curves; b) Thickness sensitivity ( $\psi$ ) curves at four separations; (numbers refer to levels of measurement, for other symbols see text)

12. ábra. 15 m vastag bauxitrétegben, a nagyellenállású aljzat felett különböző szinteken végzett Schlumberger-szondázások

a) Látszólagos fajlagos ellenállás ( $\rho_a$ ) görbéi; b) Vastagság érzékenység ( $\psi$ ) görbéi négy terítési távolságra (az ábrán a számok a szinteket jelölik, a többi jel magyarázatát lásd a szövegben)

Рис. 12. Зондирования установкой Шлюмберже в пределах бокситовой залежи на различных вертикальных расстояниях от высокоомной почвы.

a) Кривые кажущихся удельных сопротивлений ( $\rho_a$ ).

b) Кривые чувствительности к мощности ( $\psi$ ) для четырех различных разнов.

perience gained from the underground measurements carried out up to now it seems that measuring techniques with  $\psi_i, \phi_i < 0.1$  are not worth applying.

In the interpretation of soundings, sensitivities belonging to several separations should be considered. Statistical interpretation methods [GOLC' MAN 1976, SALÁT et al. 1982] provide a possibility for that both in the period of planning and in the interpretation of field measurements. Such a study is currently being prepared.

## REFERENCES

- BREITZKE M., DRESEN L., CSÓKÁS J., GYULAI Á., ORMOS T. 1987: Parameter estimation and fault detection by three-component seismic and geoelectrical surveys in a coal mine. *Geophysical Prospecting* **35**, 7, pp. 832–863
- CSÓKÁS J. 1974: Detection of tectonic disturbances associated with a coal bed by geoelectrical measurements in mine drifts. *Acta Geodaet., Geophys. et Montanist. Acad. Sci. Hung. Tomus* **9**, (1–2), pp. 111–119
- CSÓKÁS J., DOBRÓKA M., GYULAI Á. 1986: Geoelectric determination of quality changes and tectonic disturbances in coal deposits. *Geophysical Prospecting* **34**, 7, pp. 1067–1081
- DOBRÓKA M., GYULAI Á., TAKÁCS E. 1987a: Development of a mathematical physical model to determine the spatial position of coal seams (in Hungarian). Final research report, UHI, Department of Geophysics, Miskolc
- DOBRÓKA M., GYULAI Á., ORMOS T., TAKÁCS E. 1987b: Development of combined seismic-geoelectric in-mine geophysical methods (in Hungarian). Research report, UHI, Department of Geophysics, Miskolc
- EGERSZEGI P. 1980: Effect of the location of electrodes and of the use of two feeding circuits with geoelectric soundings (in Hungarian with English summary). *Magyar Geofizika* **XXI**, 5, pp. 185–192
- GOLC'MAN F. M. 1976: Komplexinterpretation bei der Lösung inverser geophysikalischer Aufgaben. *Gerlands Beitr. Geophysik, Leipzig*. **85**, 5, pp. 379–384
- GYULAI Á. 1979: Evaluation of mine roadway soundings in coal bed series (in Hungarian with English summary). *Magyar Geofizika* **XX**, 4, pp. 142–148
- GYULAI Á. 1985: Three dimensional geoelectric measurements in mines for the determination of the protective layer. *Annales, Universitates Scientiarum Budapestiensis de Rollando Eötvös Nominatae, Sectio Geophysica et Meteorologica, Tomus I–II*, pp. 167–181
- KIRÁLY E., SZIGETI G. 1985: New method for the exploration of solid mineral deposits of complex tectonics. *ELGI Annual Report 1985*, pp. 197–200
- KOEFOD O. 1979: Geosounding principles, I. Resistivity sounding measurements. Elsevier, Amsterdam–Oxford–New York, 276 p.
- SALÁT P., TARCSAI GY., CSEREPES L., VERMES M., DRAHOS D. 1982: Information statistical methods of geophysical interpretation (ed. P. Salát) Tankönyvkiadó, Budapest, 302 p.
- SZABÓ J., GÉRESI GY. 1983: Geoelectrical method for analysing rock mechanical events in mine-shafts. *Magyar Geofizika* **XXIV**, 4, pp. 141–147

## FÖLDALATTI EGYENÁRAMÚ MÉRÉSEK PARAMÉTERÉRZÉKENYSÉGE

GYULAI Ákos

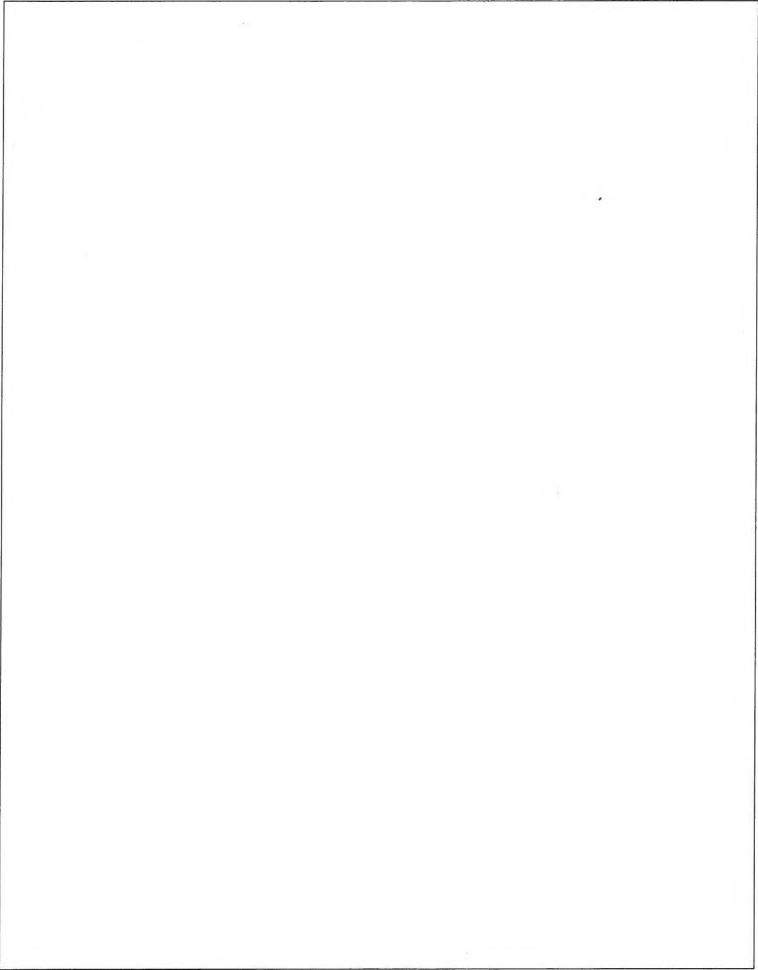
Földalatti egyenáramú mérési módszerek összehasonlításához, a kutatás megtervezéséhez célszerű az ún. paraméterérzékenységek bevezetése és alkalmazása. A mélység- (vastagság-) érzékenységek és a fajlagos ellenállás érzékenység definiálása után különböző telepes modellekre (szén, bauxit) számitott paraméterérzékenység függvényeket, majd ezek alapján a földalatti mérések néhány jellegzetességét mutatja be a dolgozat.



**ЧУВСТВИТЕЛЬНОСТЬ ПАРАМЕТРОВ ПЛАСТА ПРИ ЗОНДИРОВАНИЯХ  
МЕТОДОМ ПОСТОЯННОГО ТОКА В ПОДЗЕМНЫХ УСЛОВИЯХ**

Акош ДЬЮЛАИ

Для сопоставления методов электроразведки постоянным током в подземных условиях, для планирования исследований необходимо введение и употребление понятия, так называемой, чувствительности параметров пласта. Наряду с определением чувствительности мощности (глубины) и удельного сопротивления приводятся зависимости чувствительности параметров пласта, рассчитанные на моделях различных залежей (угля, боксита), а также некоторые особенности зондирования в подземных условиях.



This page is waiting for you!